1138

JULY 1975 MATT-1138

A SYSTEM FOR RAPID INJECTION OF METAL ATOMS INTO PLASMAS

BY

E. S. MARMAR, J. L. CECCHI
AND
S. A. COHEN

PLASMA PHYSICS LABORATORY

PRINCETON UNIVERSITY
PRINCETON, NEW JERSEY

This work was supported by U. S. Atomic Energy Commission Contract AT(11-1)-3073.

DISCLAIMER

A System for Rapid Injection of Metal Atoms Into Plasmas

E. S. Marmar, J. L. Cecchi,

S. A. Cohen

Plasma Physics Laboratory, Princeton University

Princeton, New Jersey 08540

ABSTRACT

A system for producing 300 μs bursts of 10^{17} metal atoms with 3 eV average energy is described. It is shown that this system can be successfully used to introduce impurities into CTR oriented tokamaks for transport and confinement studies.

I. INTRODUCTION

The effects of impurity ions on hydrogen plasmas are important to both present day and future CTR tokamaks.[1] Early investigations of impurity behavior relied on the presence of intrinsic impurities,[2,3,4,5] such as oxygen, carbon or iron. However, the influx of these may be neither repeatable nor constant. To remedy this source function problem more recent experiments[6,7] have used a pulsed gas method to inject impurities. Although this is a major improvement, it suffers from several drawbacks: first, thermal velocities of room temperature gases give pulse widths of approximately 3 msec. This is long compared to estimated impurity diffusion times at the edge of a plasma -- one of the processes that should be studied. Second, room temperature gases have insufficient velocity to penetrate the scrape-off region in the shadow of the limiter. This necessitates "flooding" the edge of the discharge with gas to get sufficient penetration. It has been shown[6,8] that this leads to edge cooling, an unwanted change in the plasma profile. Third, gas type impurities lost at the edge may recycle back into the plasma giving a false measure of confinement time. Fourth, there are a limited number of gases and consequently, a limited number of observable ionization states. If one could inject non-gaseous elements the larger choice of ionization states might better match plasma determined parameters such as ionization and excitation rates.

To eliminate these problems we have developed a system, based on a method first described by Friichtenicht,[9] to inject

intense (3×10^{22} particles/cm^2-sec), short (300 μs) bursts of energetic (1-20 eV) neutral metal atoms into a tokamak. The method has been investigated on a test stand and subsequently installed and operated on the Princeton Adiabatic Toroidal Compressor (ATC) Tokamak. This paper reports new phenomena associated with the method and characteristics of operation on ATC.

II. METHOD AND APPARATUS

Friichtenicht[9] has shown that high power laser irradiation of a metal film - glass interface can result in efficient vaporization of the metal and the generation of a highly directional burst of 1 to 20 eV neutral atoms. Though much work has been done on laser irradiation of solids,[10,11] there are no reported calculations for this particular energy range and geometry.

The main components of the injector system are a Q-switched ruby laser, a vacuum system (base pressure 1×10^{-7} T) and a target. The target is a 2" x 2" x .050" glass slide with 1.5 μ of a metal vacuum evaporated on one side. Usually a 500 A$^{\circ}$ Cr film is first evaporated on the slide to increase the sticking of the thick metal film. A 20 ns, 2 joule pulse from the laser is directed through a 33 cm focal length f/16 lens into the vacuum system and onto the target which is approximately 25 cm from the lens. The laser beam is incident through the glass onto the metal-glass interface. The target is moved in a plane perpendicular to the laser beam so that a number of spots can be irradiated without breaking vacuum. Figure 1 shows a photograph of a typical target after repeated shots of the laser at different locations.

III. EXPERIMENTAL RESULTS - TEST STAND

A test stand was constructed to determine the characteristics of the various components emitted from the irradiated target. In the test stand, shown in Fig. 2, a drift tube extends from the injector vacuum chamber and contains two sets of parallel plates 20 and 100 cm from the target. Electric fields up to 5000 V/cm can be applied across these plates. Magnetic fields can also be applied along the flight path in both perpendicular and parallel directions. At the end of the drift tube, 200 cm from the target, is a quadrupole mass filter (QMF) system (Extranuclear 324-9) with electron bombardment ionizer. The detector in the QMF is an off-axis, 12 stage, Be-Cu electron multiplier (EM), with its first dynode at -3KV. The signal from the EM is displayed on an oscilloscope which is triggered by the laser pulse.

The sensitivity of this detection scheme to neutral aluminum atoms has been estimated by measuring the EM gain and calibrating the combined ionizer efficiency and quadrupole transmission. This calibration has been obtained by measuring the EM signal at a known pressure of CO and ionizer current and correcting for the differences in ionization efficiencies by using measured[12] and calculated ionization cross sections.[13] For 1 eV aluminum atoms entering the ionizer on axis, and an ionizer emission current of 10 ma, the detection system has an estimated efficiency of 1×10^{-5}, (assuming that the sensitivity is proportional to the

transit time of the atom through the ionizer region).

Under various conditions, the following species have been generated by laser irradiation.

1. Neutral Atoms

For laser energy densities between 1 and 50 J/cm^2 neutral atoms were detected for aluminum, iron and copper targets. Figure 3 shows a typical oscillograph of the arrival time distribution of aluminum. A search was made for Al_2 and Al_3 but no evidence for them was found ($Al/Al_2 > 100$). Energy distributions for copper, iron and aluminum targets have been calculated from the arrival time data and are shown in Fig. 4. A Maxwellian distribution is included for comparison.

The neutral aluminum signal becomes more reproducible as the laser energy density is lowered until the point at which the metal is no longer completely vaporized from the glass, ($\varepsilon \lesssim 2$ J/cm^2). The copper signal is less reproducible than that of aluminum, even at the lower laser energy densities. The iron signal is the most reproducible. These results are summarized in Table 1. The magnitude of the neutral aluminum signal was about 10 times greater than if the aluminum vaporized off the target with a $\cos\theta$ spatial distribution.

It should be noted that the power densities used in these experiments are twice as high as in Reference 9, while the energy densities are about 1/10 as large. Hence, the energy is absorbed approximately 10 times more efficiently at higher powers, suggesting non-linear processes.

2. Ions

For energy densities on aluminum targets greater than

20 Joules/cm^2, ions are observed. This identification follows from: (1) the signal's mass dependence; (2) its independence of ionizer current; and (3) its sensitivity to electric and magnetic fields applied in the drift tube.

The ions are not formed by collisions with residual gas atoms along the flight path. This was ascertained by varying the background pressure over two orders of magnitude without changing the ion signal.

At ε = 40 J/cm^2 the ions are typically 3 times more energetic than the neutrals and 10^4 times as abundant. The ion signal is shown in Fig. 5

3. Plasma

Plasma has been detected by using the parallel plates 100 cm from the target as Langmuir probes. One plate, biased at +300 V, measured the saturation electron current, while the other, biased at -300 V, measured the saturation ion current. Figure 6 shows results from one such experiment with a copper target. (The facts that the electrons "lead" the ions and that the ion signal has structure are not understood.) Taking into account secondary electron emission from the plates, the electron current was measured to be approximately 300 times the ion current. This is consistent with well-known plasma probe behavior:

$$\left(\frac{I_{electron}}{I_{ion}}\right)_{saturation} = \left(\frac{m_{ion}}{m_{electron}}\right)^{1/2} = 350 \text{ for copper} \qquad (1)$$

The arrival time distribution at these plates shows the directed plasma energy to be 100-500 eV/ion. No corresponding signal with

the appropriate arrival time was detected at the QMF.

The absolute value of the current implies a plasma density at the plates of approximately,

$$n_p = \frac{J}{eV} \simeq \frac{10^{-5}\text{Amp}/\text{cm}^2}{1.6\text{x}10^{-19}\text{Coul/charge}\ 3\text{x}10^{5}\text{cm/sec}} \simeq 2\text{x}10^{8}\text{cm}^{-3} \qquad (2)$$

where J = ion saturation current density
v = ion thermal velocity ≃1/8 ion directed velocity

This should be contrasted with the estimated neutral density, n_o, at this point,

$$n_o(100\ \text{cm}) \simeq 10^{12}/\ \text{cm}^{-3} \qquad (3)$$

4. Excited Neutrals

For both copper and aluminum we observe signals at the QMF corresponding to energies of about 25 eV which persist independently of any sweeping electric or magnetic field, and independently of the ionizer current or QMF setting. This signal disappears at only the lowest energy densities ($\varepsilon < 2J/cm^2$). It is absent for iron.

This signal may be due to either highly excited atoms in Rydberg levels or metastable neutrals. These may cause ionization or photon emission when they impact on the interior walls of the electron multiplier enclosure. The ions or photons caused by such phenomena may strike the first dynode of the EM. (Because of the polarity of the EM, electrons cannot be the direct source of this signal.) This signal is also shown in Fig. 5.

5. Microscopic Clusters

In addition to the smooth features in the EM signal due to the various species of neutrals and ions, spikes were observed at all but the highest and lowest energy densities for aluminum ($2J/cm^2 < \varepsilon < 20\ /cm^2$) and all energy densities for copper ($1J/cm^2 < \varepsilon < 75J/cm^2$). The height, number and arrival time of the spikes each varied by factors of 2 to 3 between successive shots. This made us suspect microscopic (as opposed to atomistic) phenomena. To study the possibility of cluster formation we placed a copper slide 20 cm down-stream from an aluminum target. This copper slide acted as a collector for microscopic fragments. After repeated laser irradiation of the aluminum target, the copper collector was removed to a scanning electron microscope with x-ray micrograph capabilities. One electron micrograph is shown in Fig. 7a. An accompanying x-ray micrograph of the same area using the Al Kα line is shown in Fig. 7b. The most salient feature is cratering of the copper surface. The x-ray micrograph shows that these craters have a high concentration of aluminum in their edges. A quantitative measure of the relative aluminum concentrations between the crater edge and the general background was made by a line scan. This was folded with the size and distribution of craters to get the fraction, f, of aluminum that arrives at the collector in the form of clusters. The result is

$$f = .05 \pm .03$$

The main uncertainty arises from the statistical variation of cluster size.

From the cluster density measured in the SEM micrographs, the average number of large ($r \geq 0.5\mu$) clusters that enter the 0.1 cm^2 aperature of the QMF is estimated to be 20 per shot. This is consistent with the observed frequency of spikes in the EM signal. The energy per aluminum nucleus of the clusters was determined from the arrival time data. It varied from 0.1 to 1.0 eV/nucleus.

One contrary note must be recorded on the interpretation of spikes as clusters. The frequency of spikes from iron was about 1/10 of that for copper and aluminum. However, SEM micrographs showed that craters of approximately the same size and number were formed.

6. Photons

An STL Model 6B fast framing camera with 10 ns. exposure was used to record the time evolution of the optical signal from the initial plasma. The framing pictures showed the luminescent region expanding for 500 nanoseconds. The photon flux then decayed away with a characteristic time of about 200 nanoseconds. These data are shown in Fig. 8. The luminescent region is elliptical, having a 2mm minor diameter and about a 60% elongation in the forward direction.

No effort was made to investigate the spectral nature of the photons or the absolute amount of energy lost by radiation.

The angular distribution of the vaporized aluminum was measured in two ways. In the first method the emitted particles were collected on a glass slide downstream from the target. By optically measuring the thickness of the deposited film, the

angular distribution was determined. These results are shown in Fig. 9a. The second method involved measuring the signal strength of the EM as a function of the angle θ, between the normal to the slide and the QMF axis. Fig. 9b shows the results of this method. For angles between 7^{o} and 25^{o} the distribution remains essentially flat.

IV. EXPERIMENTAL RESULTS ON ATC

The injector system was attached to the ATC tokamak as shown in Fig. 10. The purpose of injecting into ATC was to study the diffusion of impurities in a tokamak plasma. The results of this experiment will be presented elsewhere; however, we will discuss here some relevant details of the injector technique as applied to tokamak operation. By irradiating a 1.5μ thick target with a 3 mm diameter focused laser spot size, an estimated 6×10^{17} neutral atoms are produced. Taking into account the angular distribution and the geometry of the ATC port, about 8% of the neutrals reach the plasma. For ATC (average electron densities of 1.5×10^{13} cm^{-3}) this corresponds to a 1% injected impurity density. For comparison, typical amounts of intrinsic impurities, expressed as a percentage of electron density, are listed in Table II.

Figure 11 shows a 10% increase in the line integral of the electron density when aluminum is injected. This is consistent with the 1% aluminum abundance since the average number of electrons contributed by each aluminum atom is 10. The time decay of the increased (line integral) electron density, (τ=7ms), may be due to either a rearrangement of the electron density or

finite confinement time of the injected impurity. This will be discussed in another publication.

The injected atoms are detected by observing the characteristic line radiation of the various ionization states which occur in the hot tokamak plasma. Since most lines of interest lie in the ultraviolet (100Å - 1000Å), the instrument employed for this purpose is a McPherson model 247 grazing incidence UV monochrometer located 45^{o} around the ATC torus from the injection system. Both 300 lines/mm and 1200 lines/mm gold gratings have been used with an 85^{o} angle of incidence. The detector is a Galileo Electro Optics M306 magnetic electron multiplier with sensitivity from 2Å to 1500Å. The signal from the multiplier is amplified and displayed on an oscilloscope in order to observe the time evolution of the light signal during an ATC discharge. The monochrometer is calibrated absolutely by the branching ratio method.

Typical light signals are shown in Fig. 12. These are for the $1s^2 2s(^2S_{1/2}) - 1s^2 2p(^2P^o_{3/2})$ transition of Al XI (Li-like) at 550.01Å. The spectrometer views along the minor diameter of the plasma in the midplane and the signal is averaged with a 200μsec time constant. Transitions such as these which do not involve a change in the principal quantum number are, in general, the most intense because the plasma is most effective in populating the rather low lying excited states.

The reproducibility of the light signals is good when the target is irradiated at energy densities of $10 J/cm^2$. Figure 12 contains three consecutive signals for Al XI ($550.A^{o}$). In this figure the reproducibility of the signal amplitude is approximately

±16%.

The rapid injection of 5×10^{16} neutral atoms into ATC results in a large impurity density at the edge. Calculations for the penetration depth of these particles is shown in Fig. 13. (Ionization by electron impact is assumed.) The neutrals penetrate 2 to 4 cm in from the edge before being ionized. In this narrow shell they represent up to 15% of the local electron density. Under generally quiescent plasma conditions (no large MHD kink-like modes), this large impurity density rapidly diffuses away without significantly perturbing the plasma. However, for plasma conditions with low q values near the edge, $q \leq 2.5$, the injection of impurities can cause distruptions.

The penetration of clusters into the plasma was estimated using a simple model. As a conducting cluster crosses the toroidal magnetic field, it polarizes and causes a current, $\bar{j}$, to flow around the minor circumference. (The rotational transform ensures this.) Thus there is a $\bar{j} \times \bar{B}$ force on the cluster. This brakes the cluster, stopping a 1μ radius Al sphere with 1 eV/atom directed energy in less than 2 mm. The cluster is then completely ablated within 10 μsec by electron and ion bombardment. (It should be recalled that the amount of Al reaching the plasma in the form of clusters is a small fraction of the total.)

In addition to the study of impurity diffusion we list here a number of other possible uses for this method on tokamaks.

a. Measure changes in T_i, T_e, and n_e profiles in clean and dirty plasmas.

b. Measure the penetration of the scrape-off region versus energy of the injected neutrals.

c. Catalogue new lines for high Z impurities.

d. Examine neutral beam scattering due to high Z impurities.

e. Measure charge exchange cross sections for highly stripped impurities with neutral H.

f. Measure ion temperature and temperature equilibration time using Doppler widths.

ACKNOWLEDGMENT

We wish to thank D. Dimock for several useful suggestions, V. Corso, R. Moore and E. Tolnas for technical assistance in the construction of the apparatus, and R. Shoemaker for assistance in operating ATC.

This work was supported by U. S. Energy Research and Development Administration (formerly AEC) Contract E(11-1)-3073.

REFERENCES

[1]S. O. DEAN et al, Status and Objectives of Tokamak Systems for Fusion Research. U. S. A. E. C., Wash-1295, 1974.

[2]E. HINNOV et al, Matt 251, 1964, Princeton University.

[3]D. DIMOCK et al, in Plasma Physics and Controlled Nuclear Fusion Research (Proc. 4th International Conference, Madison, Wisconsin, 1971) 1, IAEA, Vienna (1971) 451.

[4]V. I. GERVIDS and V. A. KRUPIN, ZheTF Pis. Red. 18 106-109 (20 July 1973) 106-109.

[5]V. A. VERSHKOV and S. V. MIRNOV, Nuc. Fus. 14 (1974).

[6]S. VON GOELER et al, Nuclear Fision 15 1975, (to be published).

[7]J. L. CECCHI, Bull. Amer. Phys. Soc. 19, (1974), 853, 1774.

[8]J. C. HOSEA et al, in Plasma Physics and Controlled Nuclear Fusion Research (Proc. 4th International Conference, Madison, Wisconsin, 1971) 2, IAEA, Vienna (1971), 425.

[9]J. F. FRIICHTENICHT, Rev. Sci. Instrum., 45, (January 1974), 51.

[10]J. F. READY, Effects of High Power Laser Radiation, Academic, New York (1971).

[11]C. DE MICHELIS, IEEE J. Quantium Electronics, QE-6, (1970), 630.

[12]See, for example. J. M. LAFFERTY, J. Vac. Sci. and Tech., 9, (1971), 101.

[13]W. LOTZ, Institut für Plasmaphysik Garching Bei München, IPP 1/62, (1967).

TABLE I - Reproducibility of Neutral Production

Element	Range for Best Neutral Production	Shot to Shot Reproduc.
Al	2 - 10 J/cm^2	± 10%
Cu	2 - 6 J/cm^2	± 50%
Fe	10 - 30 J/cm^2	± 5%

TABLE II - Intrinsic Impurities Found in ATC

Species	Percent of Electron Density
Oxygen	1 - 10
Carbon	0.5 - 3
Iron	.01 - 1

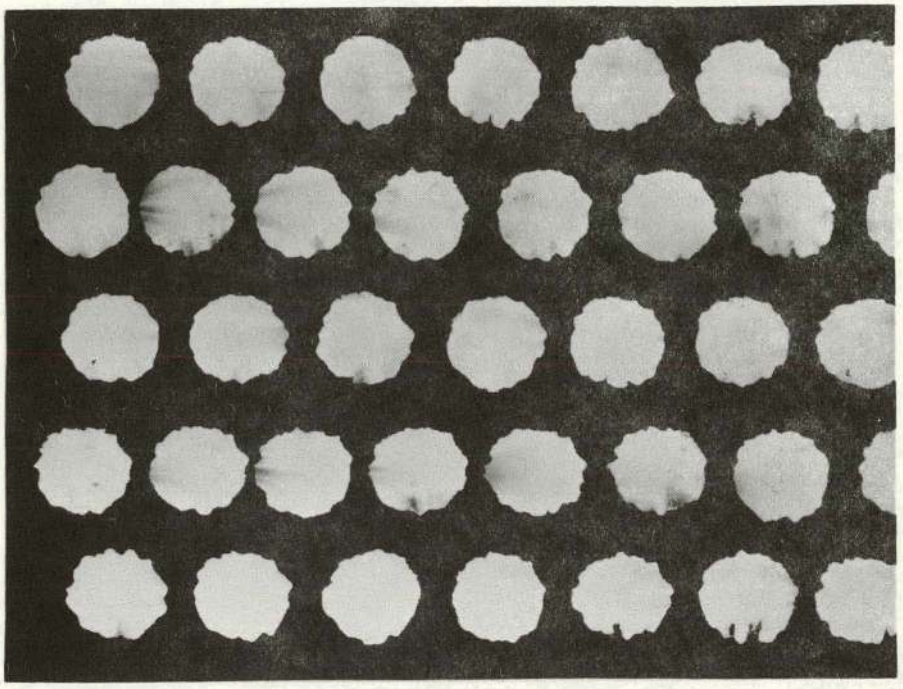

753382

Fig. 1. Al target after 36 laser irradiations. The spots are 2 mm in diameter.

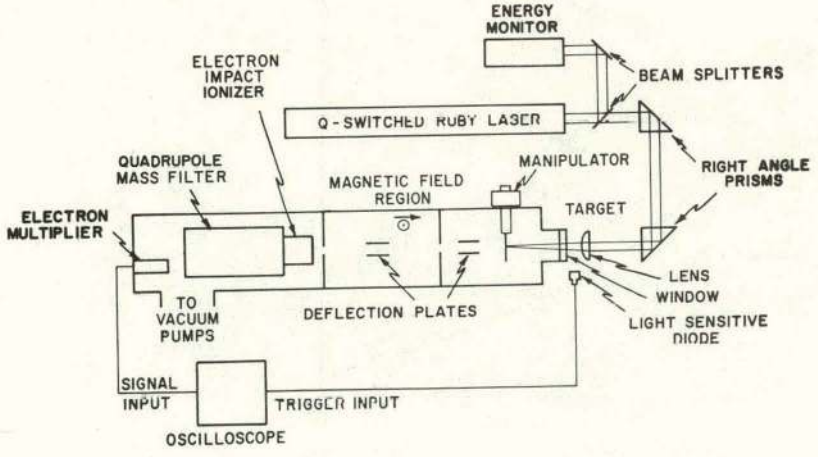

753407

Fig. 2. Schematic of Injector System and test stand. Magnetic Fields can be applied parallel to the flight path and/or perpendicular to both the flight path and the applied electric fields.

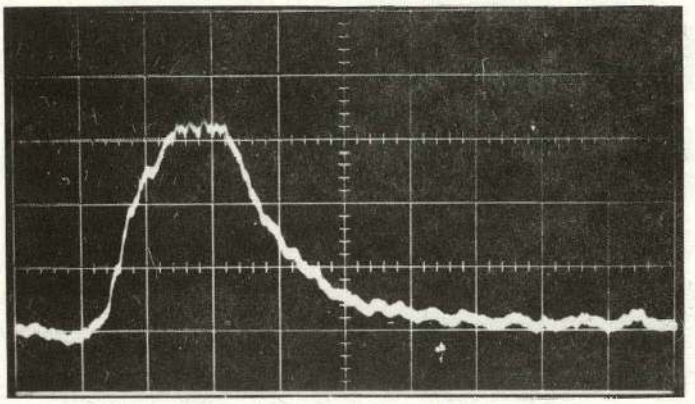

753243

Fig. 3. Oscillograph of QMF signal for Al neutral atoms. A particle with directed energy of 3 eV has an arrival time of .43 msec, Time scale is 0.2 ms/division.

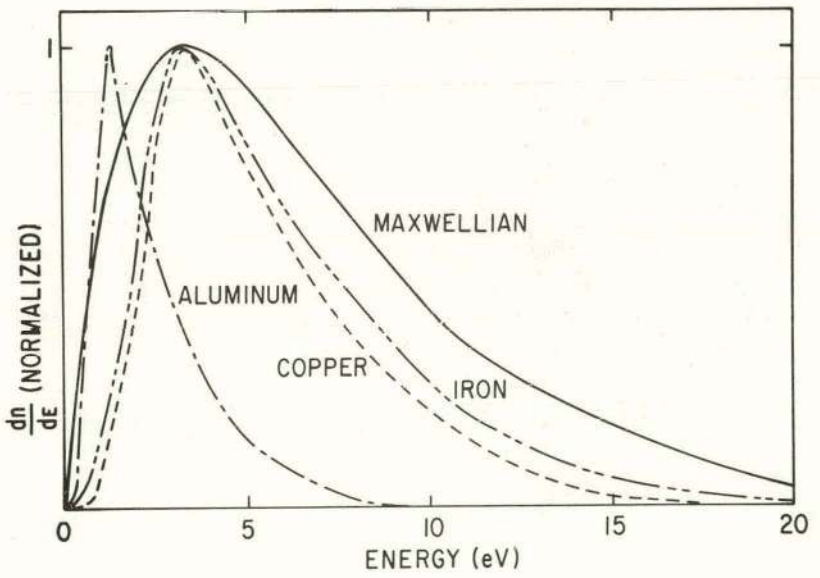

753411

Fig. 4. Energy distributions, dn/dE, for copper, iron, and aluminum. The Maxwellian distribution has a temperature of 3.3 eV.

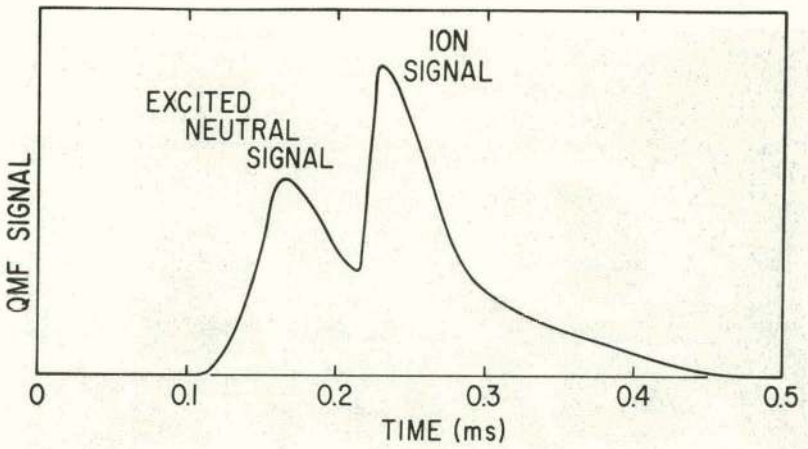

753409

Fig. 5. Excited neutral and ion signals for an aluminum burst. The laser energy density is $\varepsilon = 50$ J/cm^2.

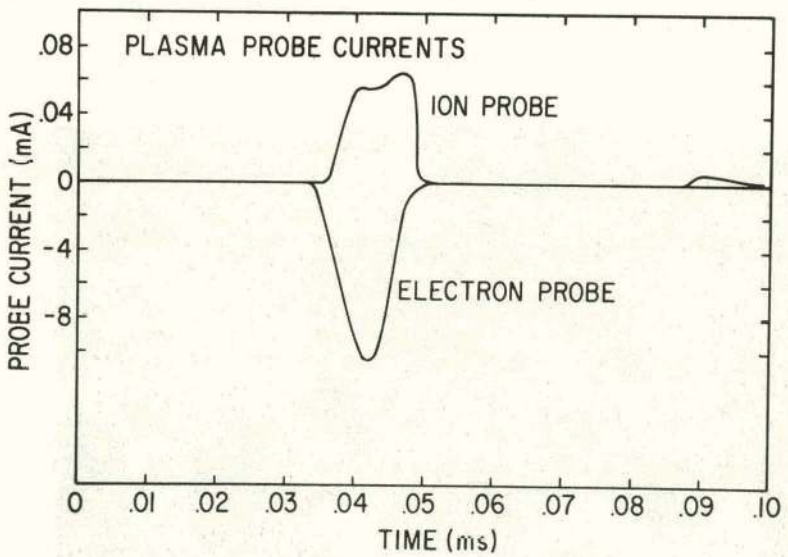

753414

Fig. 6. Saturation electron and ion Langmuir probe currents. The probes are 10 cm^2 50% transmission stainless steel meshes biased at +300 V and -300 V respectively. The plates were aligned parallel to the flight path of the plasma.

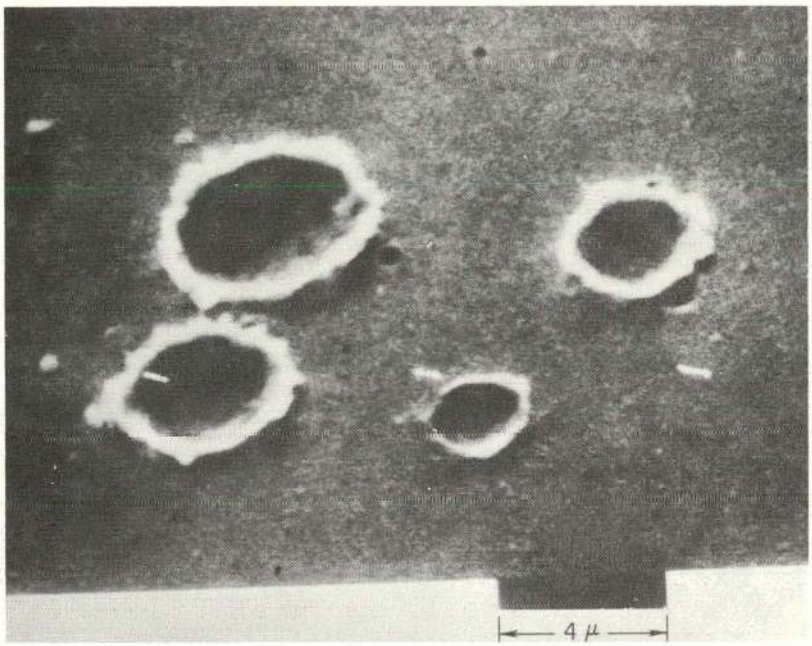

753415

Fig. 7(a) Scanning electron micrograph of aluminum bombarded copper film.

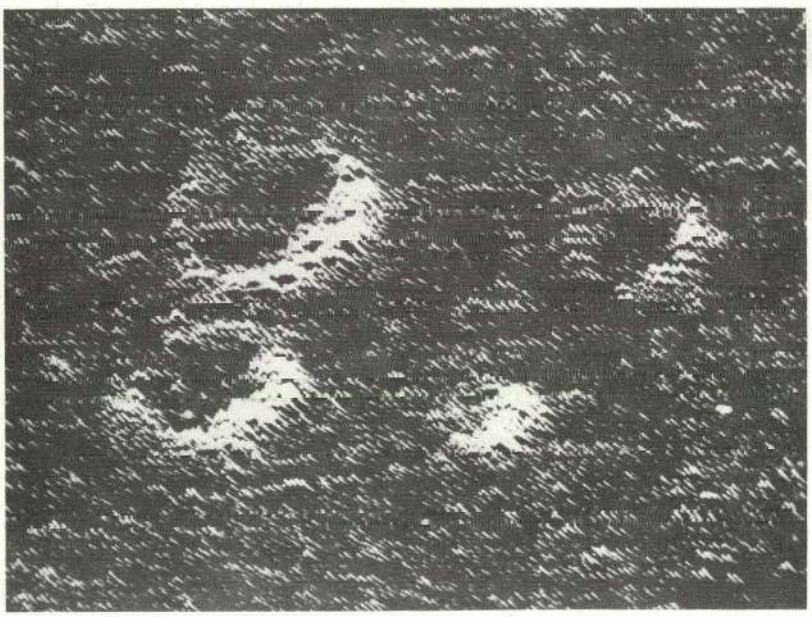

753416

Fig. 7(b) x ray micrograph of Al Kα line intensity for the same area of the copper film. The presence of aluminum is indicated by both y and z modulations.

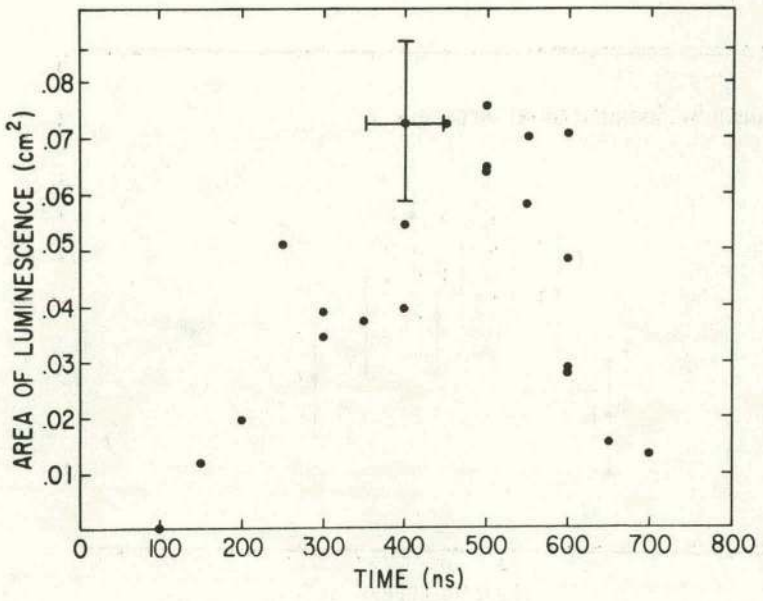

753413

Fig. 8. Cross-sectional areas of luminescent region near an aluminum target after laser irradiation. The data represent the measured areas of photographic images taken with a fast framing camera.

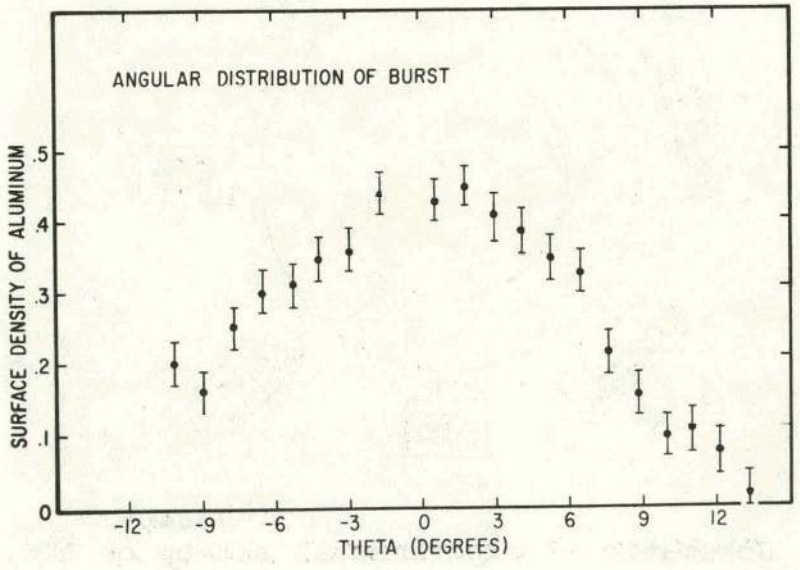

753410

Fig. 9(a) Angular distribution of vaporized aluminum collected on a glass slide.

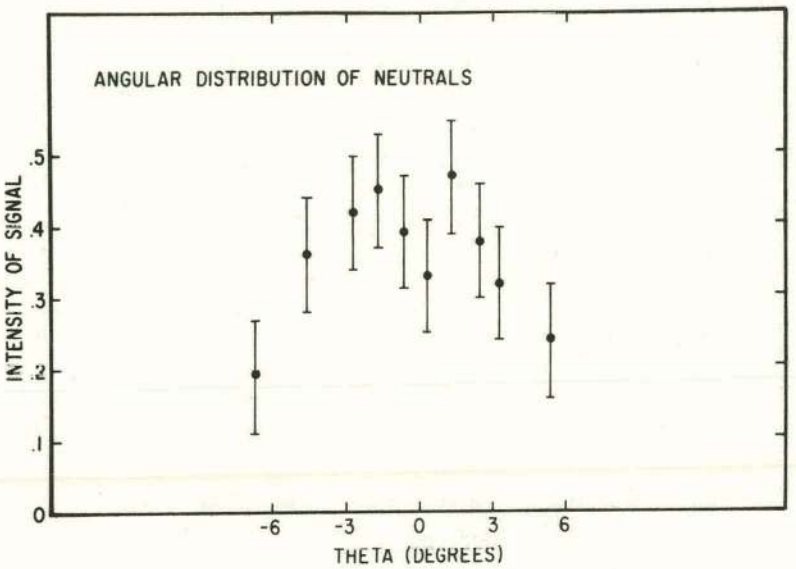

753412

Fig. 9(b) Angular distribution of aluminum neutral signal at QMF.

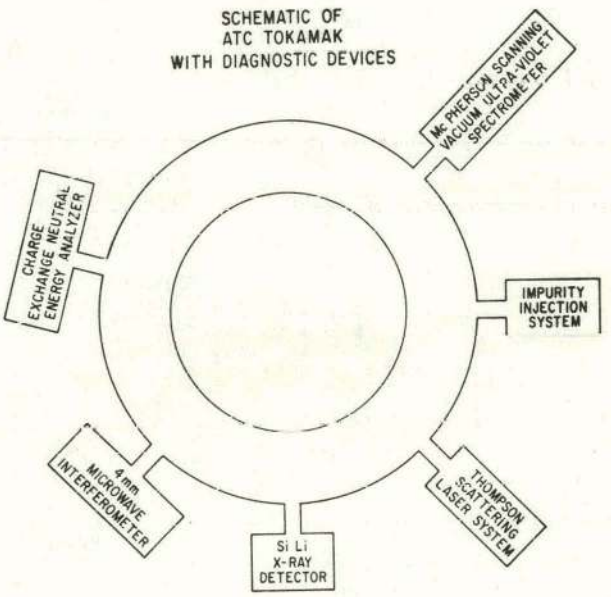

753406

Fig. 10. Schematic of experimental set-up on ATC.

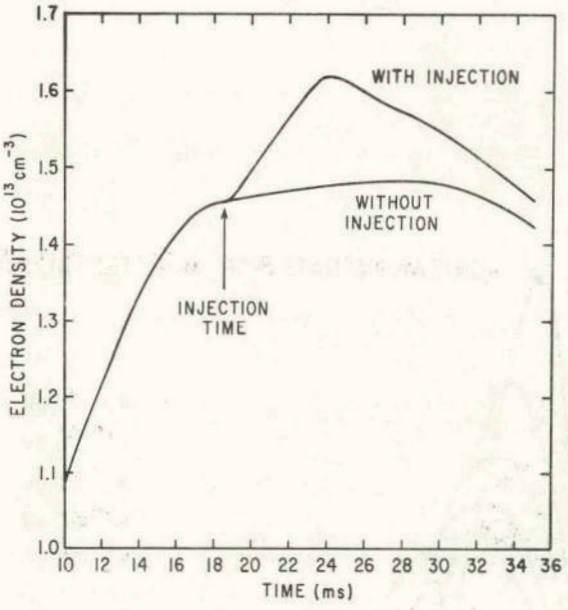

753408

Fig. 11. Line integral of electron density across a minor diameter of ATC with and without impurity injection. The measurements are made with a 4 mm microwave interferometer system.

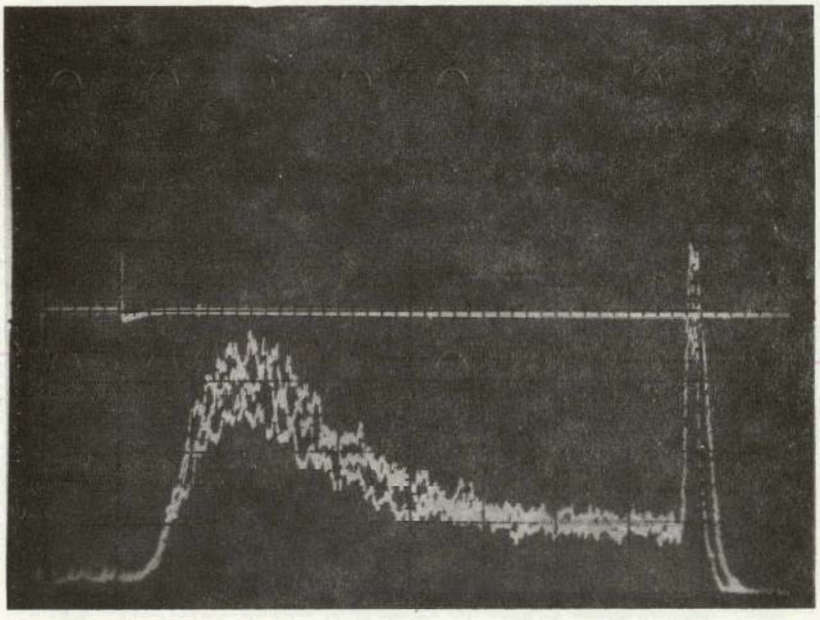

753384

Fig. 12. Time development of the line integral U.V. intensity for Al XI 550 Å line. The picture shows the overlay of signals from 3 consecutive ATC pulses. Time scale is 2.ms/division.

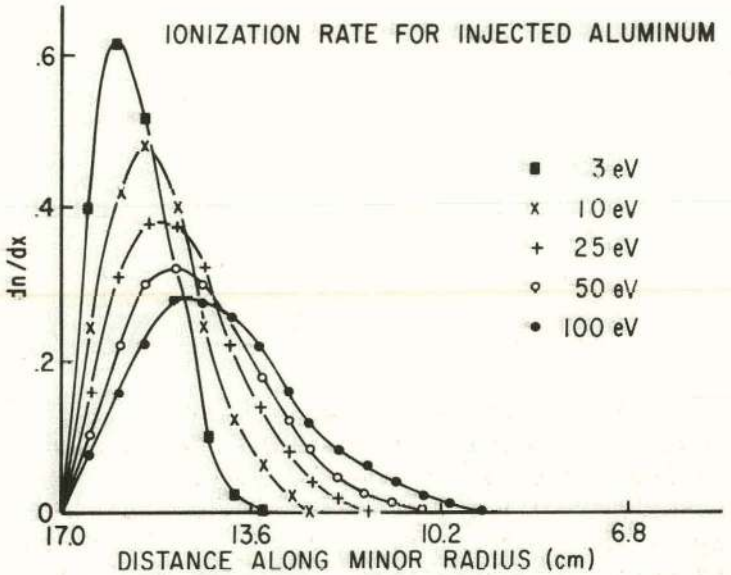

753236

Fig. 13. Calculated deposition of Al II on injection into ATC for various injection energies. Assumed electron temperature and density profiles are:

$$\left.\begin{aligned} T_e &= 750 \left(1 - \frac{r^2}{(17)^2}\right)^2 \text{ eV} \\ n_e &= 1 \times 10^{13}\left(1 - \frac{r^2}{(17)^2}\right) \text{cm}^{-3} \end{aligned}\right\} \text{r is in cm.}$$

Electron impact ionization is assumed to be the sole mechanism. The ionization rates are taken from Lotz[13].